

# DESIGN STATUS OF LHeC LINAC-RING INTERACTION REGION

J. Abelleira<sup>1,2</sup>, N. Bernard<sup>3</sup>, S. Russenschuck<sup>1</sup>, R. Tomas<sup>1</sup>, F. Zimmermann<sup>1</sup>

<sup>1</sup>CERN, Geneva, Switzerland; <sup>2</sup>EPFL, Lausanne, Switzerland; <sup>3</sup>UCLA, Los Angeles, U.S.A.

## Abstract

The ECFA-CERN-NuPECC design study for a Large Hadron electron Collider (LHeC) [1, 2] based on the LHC, considers two options, namely using a ring accelerator, similar to LEP, on top of the LHC or adding a recirculating energy-recovery linac tangential to the LHC. In order to obtain the required luminosity with an electron beam from a linac, with average lepton beam current limited to a few mA, reaching the smallest possible proton beam size is essential. Another constraint is imposed by the need to separate electron and proton beams after the collision without losing too much luminosity from a crossing angle. A further constraint is that the ep collision should occur simultaneously to pp collisions at other LHC interaction points such that the second LHC proton beam must be accommodated in the interaction region too. We present a conceptual layout using detector-integrated combination-separation dipoles and challenging Nb<sub>3</sub>Sn technology quadrupoles for focusing the colliding proton beam and providing a low-field hole to accommodate both the non-colliding proton beam and the lepton beam, and the optics for all three beams. We also discuss the optics design of the lepton final focus.

## LAYOUT

To achieve the target LHeC luminosity the colliding LHC proton and electron beams must both be squeezed to  $\beta^*$  of 0.1 m, which is about 5 times smaller than the nominal  $\beta^*$  for pp collisions in the LHC high-luminosity experiments. Design considerations for the LHeC linac-ring interaction region (IR), including the need for detector-integrated dipole magnets and the associated synchrotron radiation, have been discussed previously [3], but without offering a solution accommodating all three beams, nor incorporating any compatible magnet design.

At the LHeC proton-lepton interaction point (IP) a crossing angle of 6 mrad between the non-colliding proton beams allows enough separation to place the proton triplets. Only the proton beam colliding with the electrons is focused. A possible configuration in LHC Interaction Region 2 (IR2) is to inject the electrons parallel to the LHC beam 1 and collide them head-on with beam 2; see Fig. 1. The polarities of the present proton-beam separation and recombination dipoles (also known as “D1” and “D2”) have to be changed so as to allow for the large crossing angle at the IP. The final IR design will need to incorporate an escape line for neutral particles coming from the IP, probably requiring to split D1 into two parts separated by tens of meters. Bending dipoles around the IP are used to make the electrons collide head-on with beam 2 and to safely extract the

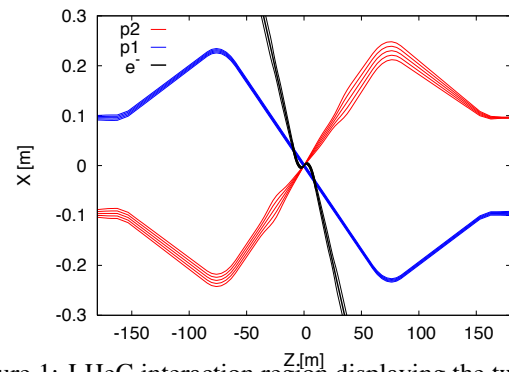


Figure 1: LHeC interaction region displaying the two proton beams and the electron beam trajectories.

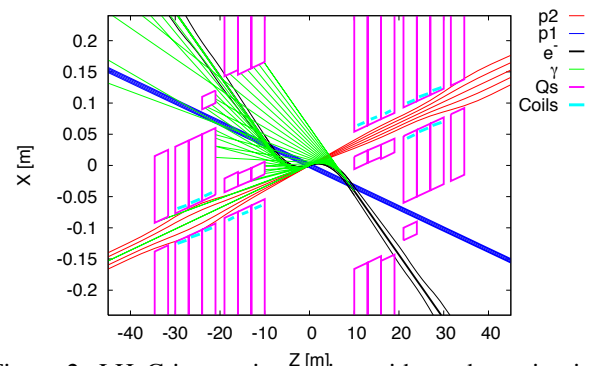


Figure 2: LHeC interaction region with a schematic view of synchrotron radiation.

disrupted electron beam after the collision. The required field of these dipoles is determined by the free length “L\*” between the last (proton) quadrupole (Q1) and the IP, by the dipole length, and by the minimum separation of the electron and the squeezed colliding proton beam at Q1. A 0.3 T field extending over 9 m allows for a beam separation of 0.07 m at the entry of Q1. This separation distance is compatible with a mirror quadrupole design for Q1 based on Nb<sub>3</sub>Sn technology, presented later. The power radiated by the electron beam at a current of 6.6 mA is 48 kW in the IR dipoles. A sketch of the LHeC IR with three beams and the electron synchrotron radiation fan is shown in Fig. 2.

## PROTON OPTICS

The colliding beam triplet starts at  $L^*=10$  m from the IP. It consists of 3 quadrupoles, the parameters of which were chosen to be consistent with Nb<sub>3</sub>Sn technology. The quadrupole aperture is computed as  $11 \max(\sigma_x, \sigma_y) + 5$  mm. The 5 mm splits into 1.5 mm for the beam pipe, 1.5 mm for mechanical tolerances and 2 mm for the closed orbit. The parameters for the first two quadrupoles correspond to the Nb<sub>3</sub>Sn magnet designs described below. The total chro-

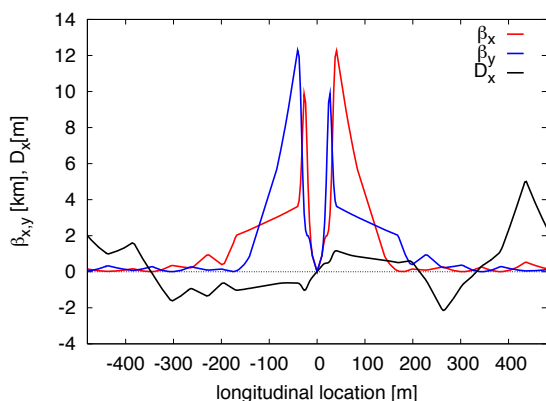


Figure 3: IR optics for the colliding proton beam.

maticity from the two IP sides amounts to 960 units, which implies the need for a dedicated chromatic correction if in parallel to LHeC running there are pp collisions in LHC IPs 1 and 5 with a  $\beta^*$  smaller than nominal. The optics functions for the colliding LHeC proton beam are shown in Fig. 3. The non-colliding proton beam travels through dedicated holes in the proton triplets quadrupoles, together with the electron beam. Its optics is similar to the existing so-called alignment optics with triplets of zero strength.

Alternatively, for the LHeC final proton quadrupoles Nb-Ti technology could be pursued instead of Nb<sub>3</sub>Sn and the  $L^*$  could also be slightly increased. The same beam crossing scheme as in Fig. 1 could be kept. All  $L^*$  values below 23 m require a cantilever supported on a large mass as proposed for the CLIC QD0 to provide sub-nanometer stability at the IP. The LHeC vibration tolerances of a few 100 nm are much more relaxed than for CLIC.

### MAGNET DESIGN

The first proton magnet viewed from the IP, called Q1, is assumed to be realized as a half quadrupole, shown in Fig. 4 (right). The second quadrupole, Q2, is a single-aperture magnet with holes, illustrated by the left picture of Fig. 4.

For both Nb-Ti and Nb<sub>3</sub>Sn superconductor technologies some limitations exist on the field gradients and the septum size that can be achieved. Fig. 5 shows the Q1 working points on the load-line considered with either superconductor technology.

For the Nb<sub>3</sub>Sn option we assume composite wire produced with the internal Sn process (Nb rod extrusions) [4]. The non-Cu critical current density is 2900 A/mm<sup>2</sup> at 12 T and 4.2 K. The filament size of 46 μm in Nb<sub>3</sub>Sn strands gives rise to higher persistent current effects in the magnet as compared with Nb-Ti magnets.

For the half quadrupole, a four layer coil must be used; see Fig. 4. The thickness of the coil is limited by the flexural rigidity of the cable, which makes the coil-end design difficult. Moreover, a thicker coil will also increase the beam separation between the proton and the electron beams. For the single aperture magnet, two interleaved sets of yoke laminations provide the necessary mechanical stability of the magnet during cooldown and excitation.

### 03 Linear Colliders, Lepton Accelerators and New Acceleration Techniques

#### A14 Advanced Concepts

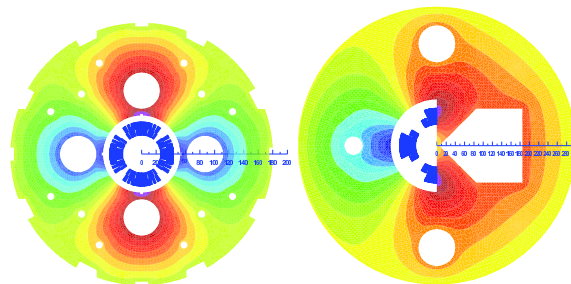


Figure 4: Cross-sections of the insertion quadrupole magnets. Left: Single aperture quadrupole Q2. Right: Half quadrupole with field-free region; design selected for Q1.

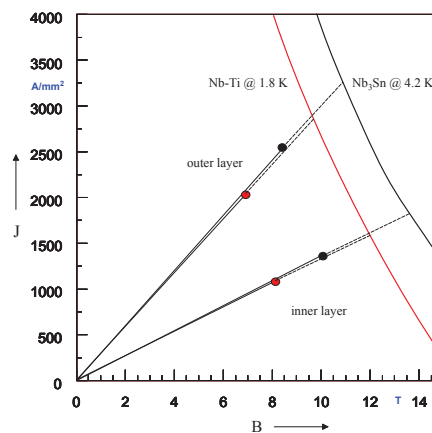


Figure 5: Working points on the load line for both Nb-Ti and Nb<sub>3</sub>Sn variants of the half quadrupole.

The results of a field computation for both the Q1 and Q2 magnet designs with Nb<sub>3</sub>Sn superconductor are summarized in Table 1. Because of iron saturation, the fringe fields in the electron beam channel are not negligible, namely 0.09 T for the single-aperture magnet and 0.5 T for the half-quadrupoles.

Table 1: Field parameters computed for the proton-beam Q1 (half-quadrupole) and Q2 (single-aperture) magnet designs based on Nb<sub>3</sub>Sn at 4.2 K

	Q2	Q1
op. current $I_{nom}$ (A)	6700	4500
field gradient $g$ (T/m)	311	175
main field $B_0$ (T)	-	4.7
op. fraction of load line (%)	83	82
e <sup>-</sup> beam field $B_{fringe}$ (T)	0.09	0.5
e <sup>-</sup> beam gradient $g_{fringe}$ (T/m)	9	25

### ELECTRON OPTICS

Two options for the electron final focus are studied, one for round beams and another for slightly flat beams, with a beam-size aspect ratio of about 2. For the electron optics a free length  $L^*=30$  m has been chosen to allow for sufficient longitudinal and transverse separation between the proton

and the electron IR quadrupoles. About 200 m are available for the electron final-focusing system between the exit of the linac and the IP. The current electron final-focus design occupies only about 90 m, which would leave space for collimation and for a beam-diagnostics section.

Coming from the IP, after traversing the separation dipole the electron beam encounters the proton triplet quadrupoles. The electron beam shares a hole with the non-colliding proton beam in the first half-quadrupole, Q1, and then travels through a dedicated hole in the cryostat of Q2. The common hole in the proton Q1 must have about 160 mm full horizontal aperture to allow for the varying separation between the electron and non-colliding proton orbit (120 mm) and for sufficient electron-beam aperture ( $\pm 20$  mm). The half-aperture Q1 magnet features a significant fringe field of 0.5 T, but improved designs, e.g., with dedicated correction, may reduce this field. Migrating to Nb-Ti technology would lower this field as well.

A round beam electron optics with  $\beta_{e;x,y}^* = 0.1$  m can be realized by a plain triplet without any sextupoles. An example optics matched to the exit of the linac is shown in Fig. 6. Upstream bending magnets complement the separation dipole so at the match the dispersion at the IP. The electron focusing quadrupoles feature moderately low gradients. The maximum value is 39 T/m. The power lost by synchrotron radiation (SR) is 25 kW, almost entirely from the last separation dipole.

Alternatively, preferably for use with unequal IP beta functions, an optics consisting of a final doublet and a chromatic correction using 4 sextupole magnets can be considered. Such a system can be based on the compact final-focus scheme proposed for future linear colliders [5]. An example optics is shown in Fig. 7. The upstream bending magnets are much stronger in order to generate the dispersion needed at the final two sextupoles. The maximum quadrupole gradient is 40 T/m, the total SR power 0.5 MW.

Table 2 compares the relative spot-size increases for the two alternative optics, considering a beam of finite momentum spread without and with the effect of synchrotron radiation [6]. The beam sizes obtained by tracking 20,000 particles without synchrotron radiation are consistent with those computed by MAD-X/PTC and MAPCLASS [7].

The beam-size increase is larger for the second optics due to the geometrical aberrations caused by the sextupoles and the much larger amount of synchrotron radiation. There are two limiting factors. The first one is  $L^*$ , which at 30 m could be too large for  $\beta_{e;y}^* = 0.05$  m. The second is the high dispersion needed in the final doublet to reduce the strength of the geometric aberrations. Doubling the length of the system, e.g. to 160 m, would allow creating a larger dispersion with less synchrotron radiation.

## CONCLUSION

A first consistent layout exists of the LHeC linac-ring interaction region, with optics for all three beams and magnet designs for the most critical, final SC proton quadrupoles. Two  $e^-$  final-focusing optics have been studied. For the

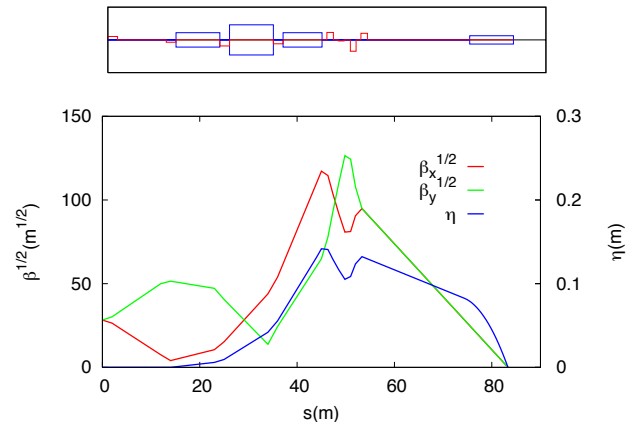


Figure 6:  $e^-$  final-focus optics for  $\beta_{e;x,y}^* = 0.1$  m based on a triplet without chromatic correction.

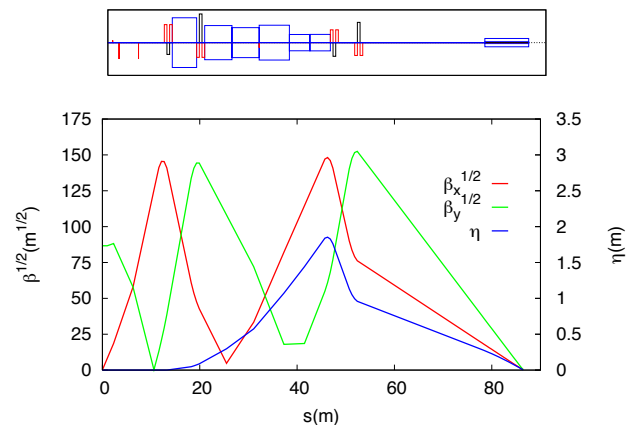


Figure 7:  $e^-$  final-focus optics for  $\beta_{e;x}^* = 0.2$  m and  $\beta_{e;y}^* = 0.05$  m, based on a doublet with local chromatic correction.

Table 2: Relative IP  $e^-$  beam-size increase with respect to  $\sigma_{0,x,y} = \sqrt{\epsilon\beta_{x,y}^*}$  for a Gaussian beam with  $\delta_{\text{rms}} = 3 \times 10^{-4}$ .

	triplet	doublet w. sext.
$\Delta\sigma_x/\sigma_{x,0}$ , no SR	10%	25%
$\Delta\sigma_y/\sigma_{y,0}$ , no SR	21%	43%
$\Delta\sigma_x/\sigma_{x,0}$ , SR	10%	34%
$\Delta\sigma_y/\sigma_{y,0}$ , SR	21%	47%

nominal momentum spread an 80-m long simple triplet solution is adequate. A larger momentum acceptance requires a longer system with chromatic correction.

## REFERENCES

- [1] LHeC web site [www.lhec.org.uk](http://www.lhec.org.uk)
- [2] LHeC Study Group, "A Large Hadron Electron Collider at CERN," LHeC-Note-2011-001 (2011)/
- [3] F. Zimmermann et al, Proc. IPAC'10 Kyoto p. 1605 (2010).
- [4] J. Parrell et al, IEEE Trans. Appl. Superc. 13, 2 (2003).
- [5] P. Raimondi and A. Seryi, Phys. Rev. Lett. 86, 3779 (2001).
- [6] G. Roy, NIMA 298, 128 (1990).
- [7] R. Tomas, CERN AB-Note-2006-017 (ABP) (2006).